

# Self-Assembly of HEK Cell-Secreted ApoE Particles Resembles ApoE Enrichment of Lipoproteins as a Ligand for the LDL Receptor-Related Protein<sup>†</sup>

Mary Jo LaDu,<sup>‡</sup> W. Blaine Stine, Jr.,<sup>§</sup> Masaaki Narita,<sup>||</sup> Godfrey S. Getz,<sup>⊥</sup> Catherine A. Reardon,<sup>⊥</sup> and Guojun Bu<sup>\*,||</sup>

Department of Anatomy and Cell Biology, University of Illinois at Chicago, Chicago, Illinois 60612, Process Sciences—Protein Analytics, Abbott Bioresearch Center, Worcester, Massachusetts 01605, Department of Pediatrics and Department of Cell Biology and Physiology, Washington University School of Medicine, St. Louis, Missouri 63110, and Department of Pathology, University of Chicago, Chicago, Illinois 60637

Received September 1, 2005; Revised Manuscript Received November 8, 2005

**ABSTRACT:** Recent studies have shown that the lipidation and assembly state of apolipoprotein E (apoE) determine receptor recognition and amyloid- $\beta$  peptide (A $\beta$ ) binding. We previously demonstrated that apoE secreted by HEK cells stably expressing apoE3 or apoE4 (HEK-apoE) binds A $\beta$  and inhibits A $\beta$ -induced neurotoxicity by an isoform-specific process that requires apoE receptors. Here we characterized the structure of HEK-apoE assemblies and determined their receptor binding specificity. By chromatography, HEK-apoE elutes in high molecular mass fractions and is the size of plasma HDL, consistent with a multiprotein assembly. No lipid was associated with these apoE assemblies. Several methods for analyzing receptor binding indicate that HEK-apoE is a ligand for low-density lipoprotein (LDL) receptor-related protein (LRP) but not the LDL receptor. This suggests that self-assembly of apoE may induce a functional conformation necessary for binding to LRP. Our results indicate that, in addition to lipid content, the assembly state of apoE influences A $\beta$  binding and receptor recognition.

Apolipoprotein E (apoE)<sup>1</sup> is a 34 kDa glycoprotein that is a surface component of various plasma lipoprotein particles including chylomicron remnants,  $\beta$ -migrating VLDL ( $\beta$ -VLDL), LDL, and a subclass of HDL (reviewed in ref 1). ApoE mediates high-affinity binding of apoE-containing lipoproteins to cell surface endocytic receptors during the transport and metabolism of plasma cholesterol (Chol) and triglycerides (TG) (1, 2). In the central nervous system (CNS), apoE is the primary apolipoprotein in the HDL-like lipoprotein particles in cerebral spinal fluid (CSF) and in the discoidal particles secreted by astrocytes in vitro (reviewed in ref 3). In humans, apoE exists in three isoforms that differ by a single amino acid at two polymorphic sites (E2 = Cys<sup>112</sup>, Cys<sup>158</sup>; E3 = Cys<sup>112</sup>, Arg<sup>158</sup>; and E4 = Arg<sup>112</sup>, Arg<sup>158</sup>). The  $\epsilon$ 4 allele of apoE is a major risk factor for

Alzheimer's disease (AD) (4, 5), suggesting that regulation of apoE expression and/or metabolism in the CNS may contribute to the pathogenesis of AD. While the mechanism by which apoE4 functions as an AD risk factor is not known, several hypotheses have been proposed. One possibility is an apoE isoform-specific response to brain injury (6, 7) and neuronal regeneration, a hypothesis supported by the observation that apoE3- but not apoE4-containing lipoproteins stimulate neurite outgrowth (8–11). Alternatively, apoE-containing lipoproteins may interact with amyloid- $\beta$  peptide (A $\beta$ ) at several mechanistic levels. First, apoE may modulate the clearance of A $\beta$  by forming a complex with the peptide that is then cleared by one or more of the numerous apoE receptors present on neurons or glial cells (12–15). Indeed, apoE3 has been shown to have a higher affinity for the peptide than apoE4, particularly when measured by the formation of an SDS-stable complex (16–18). Second, apoE affects the deposition of amyloid. AD patients with one or two alleles of  $\epsilon$ 4 exhibit a dose-dependent increase in total amyloid plaque burden compared to AD patients lacking  $\epsilon$ 4, an observation reproduced by crossing apoE null and human apoE transgenic mice with APP transgenic mice (19–21).

ApoE-containing lipoproteins bind members of the LDL receptor (LDLR) gene family. ApoE associated with LDL (2, 22) and DMPC vesicles (23) acts as ligands for the LDLR. In contrast, only apoE-enriched  $\beta$ -VLDL and recombinant apoE act as ligands for LDLR-related protein (LRP) (24–27). LRP is a large multifunctional receptor that binds and endocytosis over 30 structurally and functionally distinct ligands (26, 28–30) and is expressed abundantly in the liver and CNS. In addition to LRP, apoE-enriched lipoproteins have been shown to be ligands for other members of the

<sup>†</sup> This work was supported by NIH Grants NS37525 (G.B.), AG19121 (M.J.L.D.), and NS520138 (G.S.G. and C.A.R.), American Health Assistance Foundation ADR97006 (G.S.G. and C.A.R.), and the Charles Walgreen, Jr., Fund (M.J.L.D.). G.B. is an Established Investigator of the American Heart Association.

\* To whom correspondence should be addressed: phone, (314) 286-2860; fax, (314) 286-2894; e-mail, bu@wustl.edu.

<sup>‡</sup> University of Illinois at Chicago.

<sup>§</sup> Abbott Bioresearch Center.

<sup>||</sup> Washington University School of Medicine.

<sup>⊥</sup> University of Chicago.

<sup>1</sup> Abbreviations: apoE, apolipoprotein E; A $\beta$ , amyloid- $\beta$  peptide; AD, Alzheimer's disease; LDL, low-density lipoprotein; HDL, high-density lipoprotein; VLDL, very low density lipoprotein; DMPC, dimyristoylphosphatidylcholine; LDLR, LDL receptor; LRP, LDL receptor-related protein; HSPG, heparan sulfate proteoglycan; RAP, receptor-associated protein; MEF, mouse embryonic fibroblasts; SEM, standard error of the mean; CNS, central nervous system; CSF, cerebral spinal fluid; SEC, size exclusion chromatography; FPLC, fast protein liquid chromatography; EM, electron microscopy.

LDLR gene family such as megalin/LRP2 (31), the VLDL receptor (32), and apoE receptor 2 (apoER2) (33, 34). The ability of apoE-containing lipoproteins to bind multiple members of the LDLR gene family suggests that apoE recognizes a common structural motif that is present within the ligand-binding regions of these receptors. However, apoE-containing lipoproteins also exhibit a differential affinity for members of the LDLR family, suggesting that the conformation of apoE affects its receptor-binding specificity.

We previously demonstrated that apoE particles secreted by HEK-293 cells stably transfected with human apoE3 or apoE4 cDNA (HEK-apoE) differentially form an SDS-stable complex with A $\beta$ , a property HEK-apoE shares with apoE associated with plasma lipoproteins (16, 17). Specifically, HEK-apoE3 and plasma VLDL-containing apoE3 bind A $\beta$  with a higher affinity than apoE4 (16, 17). However, apoE3 and E4 purified from HEK-apoE and plasma VLDL by a process that includes delipidation and denaturation or purchased from a commercial vendor exhibit a comparable, lower affinity for A $\beta$  (17, 18, 35). It was assumed in our earlier publications that small amounts of lipid associated with these HEK-apoE "particles" facilitated the adoption of a favorable conformation for isoform-specific interaction with A $\beta$ . To further investigate the molecular determinants that dictate the function of apoE-containing particles, we analyzed the structure, composition, and apoE receptor binding affinity of HEK-apoE. We found that while HEK-apoE was secreted as a high molecular mass assembly, was the size of plasma HDL, and measured 12 nm in size by EM analysis, HEK-apoE is virtually lipid-free. We demonstrate that these apoE assemblies are ligands for LRP but not LDLR. These results suggest that the conformation of apoE-enriched lipoproteins and the conformation of apoE induced by its own self-assembly both result in recognition by LRP. We further infer that the *in vitro* secretory process of HEK cells favors the adoption by apoE of a conformation that allows for the isoform-specific interaction with A $\beta$  and selective affinity for apoE cell surface receptors.

## EXPERIMENTAL PROCEDURES

**Materials.** Receptor-associated protein (RAP) was isolated and purified from a glutathione *S*-transferase fusion protein expressed in *Escherichia coli*, as described previously (26). *N*-Succinimidyl 3-(4-hydroxy-5-[<sup>125</sup>I]iodophenyl)propionate (Bolton and Hunter reagent) was purchased from Amersham (Oakville, Canada). Cytochrome *c*, TCA, and PBS were from Sigma Chemical Co. (St. Louis, MO). BSA (fraction V) and Pronase were from Calbiochem-Novabiochem Corp. (La Jolla, CA). PD-10 Sephadex columns and Sepharose 6 columns were from Pharmacia Biotech (Uppsala, Sweden). Tissue culture media were from GibcoBRL (Grand Island, NY).

**Preparation of HEK-apoE Particles.** As previously described, HEK-293 cells were stably transfected with cDNAs encoding human apoE3 or apoE4. Serum-free conditioned media were harvested, concentrated to 500  $\mu$ g/mL, and dialyzed (10 kDa cutoff membrane) in PBS (HEK-apoE) (16, 36).

**SDS-PAGE.** Five micrograms of HEK-apoE was added to LDS sample buffer under nonreducing conditions, loaded on a 4–12% BIS-TRIS NuPAGE gel (Invitrogen), and

electrophoresed at 160 V for 60 min. Gels were stained with Simply Blue Coomassie stain (Invitrogen) according to manufacturer's protocol. Molecular mass values were determined using protein standards (BenchMark, Invitrogen).

**HEK-apoE Molecular Mass Determination by Calibrated Size Exclusion Chromatography (SEC).** Chromatography was performed using a low dead volume HPLC equipped with biocompatible solvent delivery (Dynamax, Rainin Instruments) and UV detection (UV-1, Rainin Instruments). A single Superose 6 column was equilibrated in PBS, and 100  $\mu$ L samples were injected and chromatographed at a flow rate of 0.4 mL/min. Column parameters used for calculation of  $K_{av}$  values were obtained from the manufacturer except column exclusion limit (void volume) that was measured using blue dextran (Pharmacia) and inclusion volume which was measured using acetone diluted 1:100 in PBS.

Molecular mass and Stokes radius (size) values were calculated on the basis of comparison of the HEK-apoE elution volume:

$$K_{av} = \frac{V_e - V_o}{V_t - V_o}$$

where  $V_e$  = elution volume for the protein,  $V_o$  = Superose 6 void volume, and  $V_t$  = total Superose 6 bed volume.  $K_{av}$  values were determined for a panel of eight proteins (Sigma) with known molecular mass values between 11 and 443 kDa: apoferritin, 443000 Da;  $\beta$ -amylase, 200000 Da; alcohol dehydrogenase, 150000 Da; bovine serum albumin, 66000 Da; ovalbumin, 42700 Da; carbonic anhydrase, 28980 Da; myoglobin, 17000 Da; cytochrome *c*, 11393 Da. A standard curve was generated plotting the log molecular mass vs  $K_{av}$ . HEK-apoE molecular mass was calculated using the following equation representing the exponential fit of the data:

$$y = 2.3133e^{0.07 - 10.56x} \quad (R^2 = 0.99391)$$

**Gel Filtration Chromatography.** As previously described, 1.0 mL of concentrated HEK-apoE was isolated by SEC using fast protein liquid chromatography (FPLC) with tandem Superose 6 columns (Amersham Pharmacia) in 0.02 M sodium phosphate, pH 7.4, with 50 mM NaCl, 0.03% EDTA, and 0.02% sodium azide (flow rate 0.4 mL/min) (37). Eighty 400  $\mu$ L samples were collected for analysis. Fractions 35–45 were concentrated and pooled for further analysis.

**Western Blots.** Laemmli buffer (2 $\times$  nonreducing) (4% SDS, no  $\beta$ -mercaptoethanol) was added to SEC fractions, boiled for 5 min, and either (1) spot blotted and probed with apoE antiserum (obtained by immunizing rabbits with apoE purified from human serum) or (2) electrophoresed (on selected fractions) on 10–20% SDS/Tricine gels, transferred to Immobilon-P membranes (Millipore Corp.), and probed with apoE antiserum.

**Electron Microscopy (EM).** Pooled fractions 35–45 of HEK-apoE isolated by SEC were examined by using the Philips CM10 electron microscope at the Electron Microscopy Core Facility of the University of Chicago as described previously (37, 38). The diameters of 100 intact particles from an enlarged photomicrograph were measured by using a micrometer lens and expressed as the mean  $\pm$  standard error of the mean (SEM).

**Ultracentrifugation.** As previously described, 1.0 mL of concentrated HEK-apoE was separated on 3–20% sodium bromide single-spin gradients by centrifugation at 38000 rpm in an SW41 Ti rotor for 66 h at 15 °C. Thirty 400  $\mu$ L fractions were collected and dialyzed against Tris-buffered saline before analysis (37, 39). In addition, the HEK-apoE media were adjusted to a density of 1.25 g/mL with sodium bromide to isolate total lipoproteins.

**Lipid Analysis.** Total cholesterol (Chol), triglyceride (TG), and phospholipids (PL) were measured enzymatically using commercial kits (Boehringer Mannheim for TC and TG; Waco, Richmond, VA, for PL). The sensitivity limit of these kits is <1 ng/mL.

**Cell Culture.** Wild-type mouse embryonic fibroblasts (MEF-1 cells), fibroblasts homozygous for disruption of the LRP gene (MEF-2 cells), fibroblasts homozygous for disruption of the LDLR gene (MEF-3 cells), and fibroblasts homozygous for disruption of both LRP and the LDLR genes (MEF-4 cells) were kindly provided by Joachim Herz (University of Texas Southwestern Medical Center at Dallas). MEF cells were cultured at 37 °C in a humidified incubator with 5% CO<sub>2</sub> in DMEM supplemented with 10% fetal calf serum.

**LDLR Assay.** The LDLR binding assays were performed essentially as described (23). Human LDL was isolated from the plasma of normal fasting subjects and radiolabeled by the iodine monochloride method. Recombinant apoE3 or apoE4 was mixed with dimyristoylphosphatidylcholine (DMPC, Sigma) at a ratio of 1:3.75 (w/w). Normal human fibroblasts were cultured for 1 week prior to the binding assays.

**Protein Iodination.** HEK-apoE was iodinated using the Bolton and Hunter reagent (Amersham) according to manufacturer's instructions. Briefly, 20  $\mu$ g of SEC-isolated HEK-apoE3 or HEK-apoE4 was radiolabeled with 500  $\mu$ Ci of N<sub>2</sub>-dried *N*-succinimidyl 3-(4-hydroxy-5-[<sup>125</sup>I]iodophenyl)-propionate and kept at 4 °C for 90 min with occasional manual mixing. The reaction was completed by quenching with 0.4 M glycine buffer and passed through a PD-10 Sephadex column to separate the labeled peptide from unincorporated isotope. Specific radioactivities were 5–10  $\mu$ Ci/ $\mu$ g of protein.

**Ligand Degradation Assays.** Assay buffer for <sup>125</sup>I-apoE binding and degradation was DMEM containing 6 mg/mL BSA and 5 mM CaCl<sub>2</sub>. Cellular degradation assays were performed by incubating cells in assay buffer containing <sup>125</sup>I-apoE (5 nM) in the absence or presence of unlabeled RAP (1  $\mu$ M). This concentration of RAP is sufficient to inhibit ligand binding to both LRP and the LDLR. After incubation at 37 °C for 4 h, the overlying media were removed and precipitated with TCA. Degradation of ligand was defined as the appearance of TCA-soluble radioactivity in the overlying media. Noncellular degradation of <sup>125</sup>I-apoE was determined in parallel dishes that did not contain cells and was subtracted from each point. All experiments were repeated at least three times. Data are presented as the mean  $\pm$  SEM.

**Single Cycle Endocytosis.** Single cycle endocytosis assay was performed essentially as described previously (40). Briefly, initial binding was performed with <sup>125</sup>I-apoE3 (5 nM) at 4 °C for 1.5 h. Cells were then washed three times with DMEM containing 6 mg/mL BSA and 5 mM CaCl<sub>2</sub>, followed by incubation at 37 °C in the presence of 1  $\mu$ M RAP. At selected intervals, buffer overlying each monolayer

was removed and subjected to TCA precipitation. Dishes were then quickly chilled on ice, and cell monolayers were treated with 0.25% (w/v) Pronase in PBS for 30 min at 4 °C to remove residual surface-bound ligand. This treatment also detached cells from culture wells. The detached cells were then separated from buffer by centrifugation. Radioactivity associated with cell pellets represents internalized protease-resistant ligand, whereas radioactivity in the supernatant fraction represents surface protease-sensitive ligand. Degraded ligand was defined as TCA-soluble radioactivity in the overlying buffer. Each determination was performed in triplicate.

## RESULTS

**HEK-apoE Can Be Isolated as a Pure ~34 kDa Protein.** Isolation of HEK-apoE3 and HEK-apoE4 assemblies was performed using tandem Superose 6 columns equilibrated in PBS. A representative trace (Figure 1A) demonstrates that HEK-apoE eluted as a single peak with Gaussian distribution. Analysis of the peak fractions by SDS-PAGE demonstrated that the majority of the protein migrated as a single species with a molecular mass of ~34 kDa (Figure 1B). The observed value is slightly greater than the 34 kDa predicted by the apoE sequence and may be due to posttranslational modifications resulting from expression in eukaryotic HEK cells. Under nonreducing conditions dimeric HEK-apoE3 was detected (Figure 1B, arrow). As predicted, no dimer was detected for HEK-apoE4 lacking the Cys<sup>112</sup> residue necessary for intermolecular disulfide bond formation.

**HEK-apoE Migrates as a 360–390 kDa High Molecular Mass Complex As Determined by Calibrated SEC Analysis.** To compare the hydrodynamic properties of HEK-apoE3 and HEK-apoE4, samples were subjected to calibrated SEC analysis. The size of the HEK-apoE assemblies that eluted as a single peak from the Superose 6 column (Figure 1A) was estimated by calibrating the Superose 6 column using a panel of eight known proteins (Figure 2). An exponential fit to the data yielded a good predictive value ( $R^2 = 0.9939$ ). On the basis of the equation for the exponential fit, HEK-apoE3 assemblies had a calculated molecular mass of 360 kDa, and HEK-apoE4 had a calculated molecular mass of 390 kDa (Figure 2, open boxes). These results suggest a possible assembly of 10–12 apoE monomers.

**HEK-apoE3 and HEK-apoE4 Assemblies Are 8–15 nm in Size and Lipid-Poor.** Using SEC with tandem Superose 6 columns (37, 38), the size distribution of protein assemblies in conditioned media from HEK cells expressing apoE3 and apoE4 was compared to human plasma lipoproteins (Figure 3A). The major portion of the apoE in the media from HEK-apoE3 and HEK-apoE4 cells eluted in fractions 35–45, indicating an approximate size of 8–15 nm, comparable in size to plasma HDL-2 particles. This localization of apoE is confirmed by Western blot analysis of selected FPLC fractions via nonreducing SDS-PAGE (Figure 3B) with apoE3 appearing as monomer and dimer and apoE4 primarily as monomer. The small amount of apoE4 dimer likely resulted from noncovalent dimerization of apoE, and the bands smaller than the apoE monomeric size likely represent products of apoE proteolytic processing (50). The secondary apoE peak at fractions 50–60 is likely to be monomeric apoE as free proteins, such as albumin, elute in these fractions.



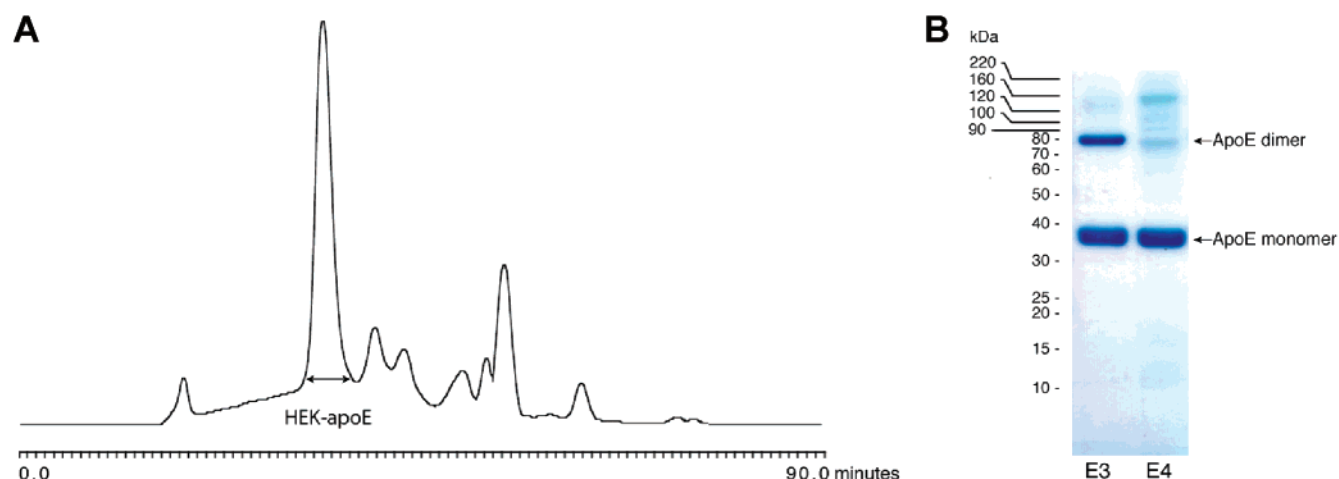


FIGURE 1: Isolation of HEK-apoE. (A) Representative Superose 6 elution profile of concentrated media from HEK cells stably transfected with the cDNA encoding human apoE isolated in PBS. Cell culture media containing secreted apoE were concentrated 50-fold and injected on Superose 6 columns at a flow rate of 0.4 mL/min. Fractions across the primary peak, detected by absorbance at  $A_{280}$ , were pooled (HEK-apoE arrows), and the protein concentration was determined spectrophotometrically. (B) Coomassie-stained SDS-PAGE analysis of HEK-apoE3 (E3) and HEK-apoE4 (E4). 5  $\mu$ g of protein was loaded under nonreducing conditions for each isoform of HEK-apoE. Molecular mass value standards were determined by protein standards (BenchMark, Invitrogen).  $\sim$ 37 kDa HEK-apoE monomer and  $\sim$ 80 kDa HEK-apoE3 dimer are indicated with arrows.

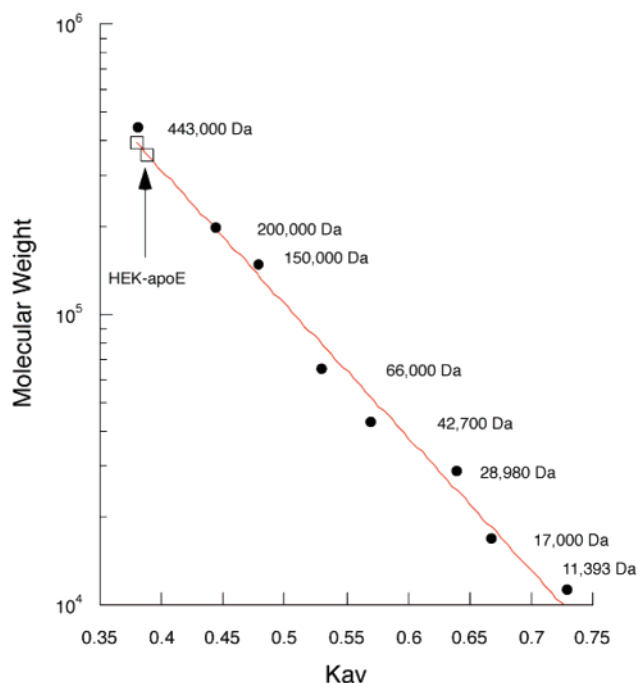


FIGURE 2: Calibrated SEC analysis of HEK-apoE. Calibration of a single Superose 6 gel filtration column. Eight proteins that ranged in size from 11 to 440 kDa were used to generate a standard curve for the gel filtration column. The molecular mass was plotted against the partition coefficient  $K_{av}$  (calculations described in Experimental Procedures). The solid line represents the best exponential fit for the data. Calculated values for HEK-apoE3 and HEK-apoE4 (open boxes) were generated using the equation representing the standard curve.

EM confirms the presence of apoE assemblies with an average diameter of  $12 \pm 1.87$  nm (Figure 4). Interestingly, the size and shapes of cell-secreted apoE assemblies are also similar to those of lipoproteins isolated from CSF (37) and  $\gamma$ -migrating, lipid-poor apoE-containing particles in plasma (12–16 nm) (41). The number of apoE monomers that make up the HEK-apoE assemblies has not yet been determined as SEC and EM analyses suggest an approximate size and morphology but not a molecular mass.

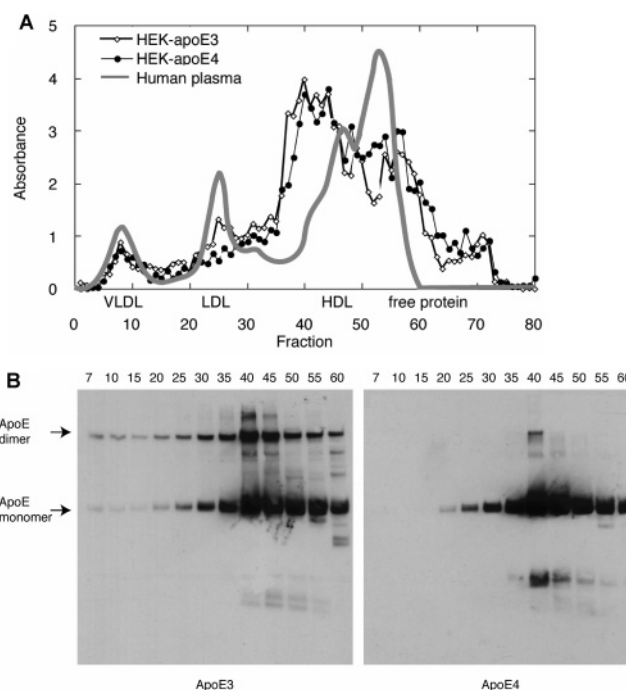


FIGURE 3: SEC profiles of HEK-apoE3, HEK-apoE4, and human plasma. (A) 1 mL of concentrated conditioned media from HEK cells expressing human apoE3 or apoE4 (HEK-apoE) was fractionated by size exclusion chromatography (SEC) using tandem Superose 6 columns and detected by absorbance at  $A_{280}$ , with the profile of human plasma included for comparison (37). ApoE immunoreactivity was determined by dot blot. Graphs are an average of  $n = 4$  separate experiments. (B) Representative Western blots of SDS-PAGE of selected HEK-apoE3 and HEK-apoE4 SEC fractions probed with apoE antisera.

Several methods of analysis were used to determine if the HEK-apoE assemblies contain lipid. First, we analyzed their density via density gradient centrifugation (37). We found that HEK-apoE distributed in the fractions corresponding to free protein, indicating an absence of lipid (Figure 5). This absence of lipid was confirmed by enzymatic analysis of the apoE-containing density gradient and SEC fractions for Chol, PL, or TG, (sensitivity limit  $<1$  ng/mL). On the basis of the

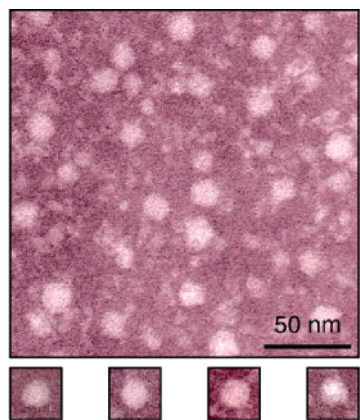


FIGURE 4: Electron microscopy analysis of HEK-apoE. Pooled fractions 35–45 of HEK-apoE isolated by SEC were concentrated, and an aliquot was placed on a carbon-coated electron microscopy grid and negatively stained with 2% phosphotungstic acid. Using a Philips CM10 electron microscope, the diameters of 100 intact particles from an enlarged photomicrograph were measured by using a micrometer lens. Representative particles are shown below, with a mean diameter of  $12 \text{ nm} \pm 1.87 \text{ SEM}$ . Results shown are for HEK-apoE3. Comparable results were observed using HEK-apoE4 (data not shown).

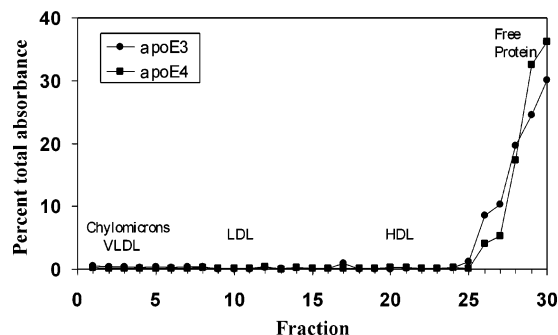
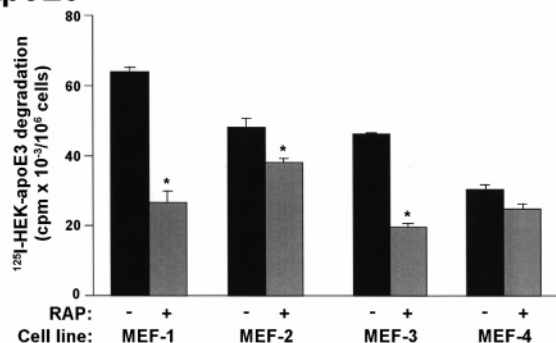


FIGURE 5: Equilibrium ultracentrifugation profiles of HEK-apoE3 and HEK-apoE4. 1 mL of concentrated HEK-apoE3 or HEK-apoE4 conditioned media was fractionated via single-spin equilibrium ultracentrifugation, and the positions of various human plasma lipoproteins are indicated for comparison. ApoE immunoreactivity was determined by dot blot. Graphs are an average of  $n = 2$  separate experiments.

concentration of apoE in the HEK-apoE-containing SEC fractions, we anticipated being able to determine the lipid profile for SEC fractions of HEK-apoE as we had for CSF and astrocyte-secreted particles (37, 38). However, no lipid was detected. Lipid was also not detected in concentrated, pooled SEC HEK-apoE fractions 35–45 nor in the  $d < 1.25$  g/mL fraction from total HEK-apoE media. Thus, some eukaryotic cells may secrete apoE3 and apoE4 assemblies with little or no lipid, unlike both CSF and astrocyte-secreted lipoproteins that contain both PL and Chol, as measured by the same enzymatic assays used for HEK-apoE (37, 38).

**HEK-apoE3 and HEK-apoE4 Assemblies Are Ligands for LRP but Not LDLR.** Previous studies have shown that apoE-containing plasma lipoproteins are ligands for the LDLR, whereas apoE-enriched  $\beta$ -VLDL, remnant particles, and recombinant apoE are ligands for LRP (2, 25, 42). To examine whether cell-secreted apoE3 and apoE4 assemblies are ligands for LDLR and/or LRP, we performed receptor-mediated ligand uptake and degradation assay using a series of genetically generated mouse embryonic fibroblast cell lines (MEF). These cell lines include (1) wild-type (MEF-1,

## A: ApoE3



## B: ApoE4

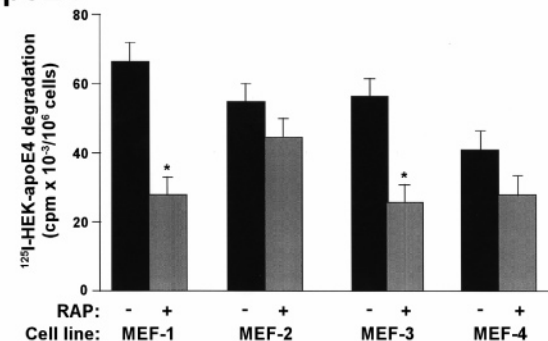


FIGURE 6: Degradation of cell-secreted HEK- $^{125}\text{I}$ -apoE3 and HEK- $^{125}\text{I}$ -apoE4 in MEF cells. MEF-1 (wild type), MEF-2 (LRP-deficient), MEF-3 (LDLR-deficient), and MEF-4 (LRP and LDLR double deficient) cells were incubated with  $^{125}\text{I}$ -HEK apoE3 (5 nM) (A) or  $^{125}\text{I}$ -HEK apoE4 (5 nM) (B) in the absence or presence of  $1 \mu\text{M}$  RAP for 4 h at  $37^\circ\text{C}$ . The degradation of  $^{125}\text{I}$ -apoE under each condition was analyzed via TCA precipitation of the overlying media. Symbols represent the average of triplicate determinations  $\pm$  SEM shown from one of three independent experiments. Nonspecific degradation of  $^{125}\text{I}$ -apoE in parallel dishes that did not contain cells was subtracted from each assay. \*,  $p < 0.05$  when compared to the column without RAP competitor.

expressing both LRP and LDLR), (2) LRP-deficient (MEF-2), (3) LDLR-deficient (MEF-3), or (4) LRP and LDLR double deficient (MEF-4) cells. In addition, we utilized RAP in these assays to ensure the specificity for LRP and LDLR. RAP functions normally within the early secretory pathway as a molecular chaperone to assist the folding and prevent premature ligand binding to the receptors during trafficking (43). The recombinant form of RAP has been used extensively as an antagonist to inhibit all known ligand interactions with members of the LDLR family (43). We chose to perform ligand uptake and degradation assays instead of saturation binding analysis because previous studies have shown that heparan sulfate proteoglycan (HSPG) is involved in the initial binding of apoE/lipoproteins, whereas apoE receptors (e.g., LRP) mediate subsequent uptake (44, 45). Thus, MEF-1, MEF-2, MEF-3, and MEF-4 cells were incubated with  $^{125}\text{I}$ -apoE3 or  $^{125}\text{I}$ -apoE4 (5 nM) in the absence or presence of  $1 \mu\text{M}$  RAP at  $37^\circ\text{C}$  for 4 h. Cellular degradation of  $^{125}\text{I}$ -apoE was assessed by TCA precipitation of overlying media after incubation with cells. We found that MEF-1 cells exhibited significant RAP-inhibitable degradation of  $^{125}\text{I}$ -apoE3 (Figure 6A). The portion of  $^{125}\text{I}$ -apoE3 degradation that was not inhibited by RAP likely reflects extracellular or cell surface degradation by secreted proteases or intracellular degradation following HSPG-mediated cellular uptake (44, 45). Interestingly, when

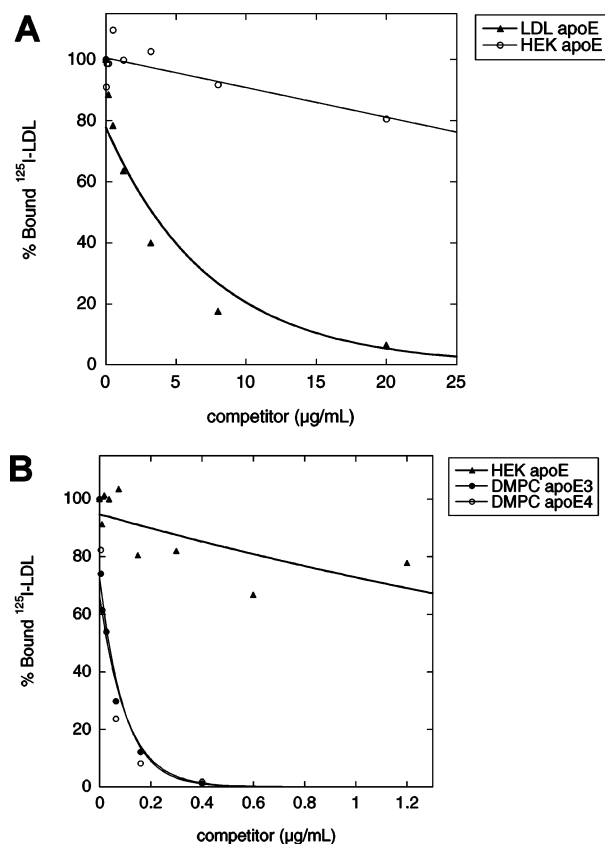


FIGURE 7: Ability of various apoE assemblies to compete with  $^{125}\text{I}$ -LDL for binding to LDLR on normal human fibroblasts. Normal human fibroblasts were incubated at 4 °C for 2 h in a medium containing 2  $\mu\text{g/mL}$   $^{125}\text{I}$ -LDL and various concentrations of unlabeled LDL (A) or DMPC-apoE3 and DMPC-apoE4 (B). The ability of HEK-apoE3 to compete with  $^{125}\text{I}$ -LDL binding was compared to those of LDL (A) and DMPC-apoE (B) at identical concentrations. Data were an average from triplicate determinations.

compared to MEF-1 cells, RAP-inhibitable degradation of  $^{125}\text{I}$ -apoE3 was comparable in LDLR-deficient MEF-3 cells but significantly less in LRP-deficient MEF-2 cells. The RAP-inhibitable degradation of  $^{125}\text{I}$ -apoE3 was minimal in MEF-4 cells, lacking both LDLR and LRP. Similar results were seen when  $^{125}\text{I}$ -apoE4 was used as the ligand (Figure 6B). Together, these results suggest that lipid-poor, cell-secreted apoE assemblies prefer LRP to the LDLR as the endocytic receptor.

As a confirmation that HEK-apoE is not a high-affinity ligand for the LDLR, the ability of HEK-apoE3 to compete for binding of  $^{125}\text{I}$ -LDL to fibroblasts was compared to LDL and DMPC-apoE3 and DMPC-apoE4 (Figure 7). Competition curves comparing LDLR binding by LDL (Figure 7A) and dimyristoylphosphatidylcholine (DMPC) vesicles (Figure 7B) indicate that both LDL and DMPC vesicles exhibit a clear dose response, with 50% binding inhibition at 3.44  $\mu\text{g/mL}$  for LDL and 0.039 and 0.036  $\mu\text{g/mL}$  for E3-DMPC and E4-DMPC, respectively. In contrast, HEK-apoE is a poor competitor for bound  $^{125}\text{I}$ -LDL and does not reach 50% binding inhibition. These results confirm that HEK-apoE is not a ligand for LDLR, as suggested by the results in Figure 6.

To confirm that cell-secreted apoE3 is internalized by LRP via a receptor-mediated endocytic pathway, we performed single cycle endocytosis analyses.  $^{125}\text{I}$ -apoE3 (5 nM) was incubated with MEF-1 cells for 1.5 h at 4 °C to allow cell

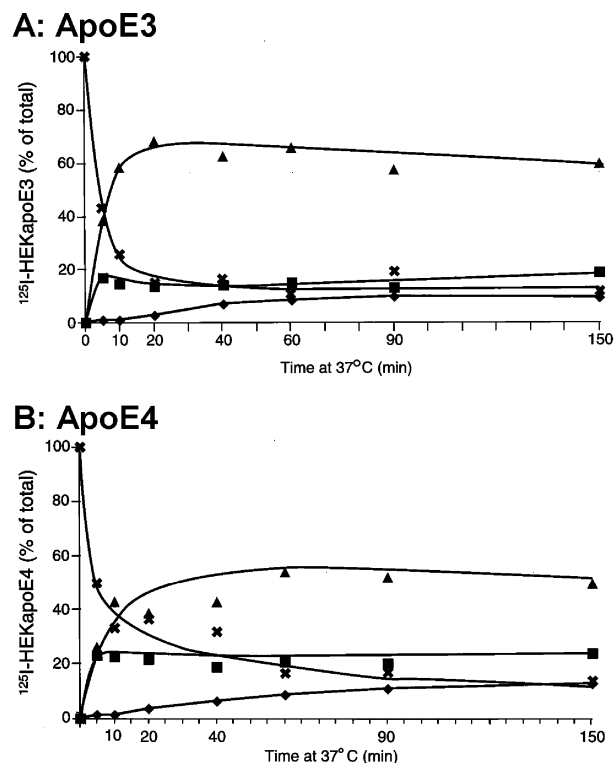


FIGURE 8: Distribution of cell-secreted HEK- $^{125}\text{I}$ -apoE3 and HEK- $^{125}\text{I}$ -apoE4 during a single cycle endocytosis in MEF-1 cells. Binding of  $^{125}\text{I}$ -HEK apoE3 (5 nM) (A) or  $^{125}\text{I}$ -HEK apoE4 (5 nM) (B) to MEF-1 cells was performed at 4 °C for 1.5 h. After washing, cells were incubated at 37 °C for selected intervals in the presence of 500 nM RAP. Overlying buffer was then removed and subjected to TCA precipitation, whereas cell monolayers were chilled and treated with Pronase. Cell surface ligand (Pronase-sensitive,  $\times$ ) and internalized ligand (Pronase-resistant,  $\blacktriangle$ ) were quantified for cells following Pronase treatment. Dissociated ligand (TCA-precipitable,  $\blacksquare$ ), as well as degraded ligand (TCA-soluble,  $\blacklozenge$ ), associated with media was also determined. Symbols represent the means of triplicate determinations.

surface binding, followed by incubation at 37 °C for selected intervals to allow ligand uptake and degradation in the presence of 1  $\mu\text{M}$  RAP. After each interval, media were removed and subjected to TCA precipitation, whereas cell monolayers were quickly cooled to prevent further ligand internalization. Cells were then treated with Pronase at 4 °C to remove residual surface ligand. The partitioning of ligand after each interval was assessed as described in the Experimental Procedures. As shown in Figure 8A, more than 70% of surface-bound ligand disappeared within the first 10 min. Concomitantly, ligand was internalized rapidly and reached a peak level at 15–20 min before subsequently declining. Ligand appeared in the media simultaneously with the disappearance of cell surface ligand. TCA-soluble radioactivity (representing degraded ligand) was detected only after a delay of 15–20 min, consistent with an endocytic trafficking and lysosomal degradation. Thus, the kinetic distribution pattern of  $^{125}\text{I}$ -apoE3 during a single cycle of endocytosis is typical of that of other ligands degraded in a receptor-mediated fashion (46). When  $^{125}\text{I}$ -apoE4 was used in the single cycle endocytosis assay, similar kinetics were observed (Figure 8B). It is interesting to note that when compared to other ligands of LRP [e.g., tissue-type plasminogen activator, or tPA (40)], a large portion of intracellular apoE remained undegraded even after 2.5 h of incubation, suggesting that



there may be an intracellular retention mechanism that is specific for apoE.

## DISCUSSION

This paper describes the structure and apoE receptor binding affinity of apoE assemblies secreted by eukaryotic cells stably expressing human apoE3 or apoE4 (HEK-apoE). Cell-secreted HEK-apoE isoforms were isolated to homogeneity by SEC, and subsequent analysis using a column calibrated for molecular mass confirmed a retention time consistent with 360–390 kDa assembly. These measured values are larger than previous reports of ~225 kDa using SEC analysis for purified recombinant and plasma apoE in aqueous solutions (47–49). However, subsequent sedimentation equilibrium analysis by analytical ultracentrifugation (AUC) of recombinant apoE demonstrated an apparent molecular mass of ~134 kDa, suggesting a tetrameric assembly, the presumed form of purified apoE (50). Although concentrating the conditioned medium may force some apoE complexes into higher order structures than would usually be obtained at in vivo concentrations, this possibility is unlikely as the concentration of apoE even after concentrating is still well below those that can result in significant aggregation under our buffer conditions (50). We have also carefully compared the elution profiles of unconcentrated and concentrated media and observed identical results. In general, the higher molecular mass values predicted by SEC analysis for apoE may be the result of nonglobular behavior during chromatographic separation. In the absence of lipid, several apoE assemblies including tetramers, octamers, and higher order apoE oligomers in dynamic equilibrium have been detected by both AUC (51) and fluorescence anisotropy (52). However, HEK-apoE migrates as a single Gaussian peak and does not exhibit the broad chromatographic distribution observed with recombinant apoE, suggesting that HEK-apoE is a stable, homogeneous multimeric assembly. As the conformation of apoE varies depending on its assembly state (50, 53), it is likely that the functional properties of these different apoE structural assemblies will also vary.

Although HEK-apoE is in the approximate size range of HDL when compared to plasma lipoproteins, these assemblies are virtually lipid-free. In vivo, apoE is detected in different lipoprotein particles. First, the most common form of apoE is as a component of several classes of plasma lipoproteins, including chylomicron remnants, LDL, and a subset of HDL. Second,  $\gamma$ -migrating, lipid-poor apoE-containing particles in plasma have been described by Huang and co-workers (41). This particle and HEK-apoE are lipid-poor/free and appear to be the same size by SEC. Third, in the CNS, HDL-like spherical apoE-containing lipoproteins are present in the CSF, and apoE-containing discoidal lipoproteins are secreted primarily by astrocytes in vitro (reviewed in ref 3).

HEK-apoE acts as a ligand for LRP but not LDLR. Members of the LDLR gene family bind apoE (26), although the conformation of apoE affects its affinity for the individual receptors. In the extreme, purification of apoE and the removal of lipid abolish its ability to bind LDLR (54), while reconstitution with lipid restores receptor-binding affinity (55). ApoE can adopt several conformations that influence its affinity for specific apoE receptors, including association

with lipoproteins and assembly state. ApoE-containing LDL and DMPC vesicles bind LDLR, but not LRP (2, 22, 23). Only apoE-enriched particles (24–26), recombinant apoE (42), and now HEK-apoE act as ligands for LRP. The common feature of these apoE assemblies that are ligands for LRP is that they are all rich in apoE. The most interesting example of receptor specificity is the  $\beta$ -VLDL. Native apoE-containing  $\beta$ -VLDL is a ligand for LDLR but not LRP. However, apoE enrichment, with either recombinant apoE or apoE extracted from native  $\beta$ -VLDL, converts these particles to a high-affinity ligand for LRP (24, 56). Therefore, the inability of apoE on the native  $\beta$ -VLDL to bind LRP is not due to any permanent modifications of apoE but rather to a lack of an apoE assembly that can be generated in the presence of higher concentrations of apoE (56). Kowal et al. have suggested that the apoE on the  $\beta$ -VLDL can be “activated” in vivo to become an LRP ligand when the  $\beta$ -VLDL acquires additional apoE while trapped in the space of Disse. Supporting this in vivo relevance, studies have shown that injection of apoE into Watanabe heritable hyperlipidemic rabbits that lack functional LDLR resulted in a significant and rapid reduction of plasma cholesterol levels (44). These results suggest that apoE enrichment of lipoprotein particles occurs in vivo, allowing apoE to facilitate cholesterol clearance via an LRP-mediated pathway. Together with our current study, it appears that the conformation of apoE induced by its enrichment on lipoprotein particles or its own self-assembly is required for recognition by LRP.

The dependence of apoE receptor recognition on the conformation of apoE is further demonstrated by two recent publications. Using reduced apoE, Ruiz and co-workers demonstrated that lipid-free apoE binds VLDLR but not LRP or LDLR (57). ApoE receptor specificity is further established by Fryer and co-workers, who demonstrated that astrocyte apoE isolated in vitro binds only LDLR and not other the LDLR family members, including LRP, ER2, and VLDLR (58). Clearly, this receptor-dependent specificity for various forms of apoE requires further investigation to determine the pattern and function of this selectivity.

In addition to functioning as ligands for LRP but not LDLR, we have previously demonstrated that HEK-apoE3 and HEK-apoE4 assemblies differentially form an SDS-stable complex with A $\beta$ , a property it shares with apoE associated with plasma lipoproteins (16, 17). Indeed, both small, lipid-poor HEK-apoE3 assemblies and large, lipid-rich plasma VLDL-containing apoE3 bind A $\beta$  with a higher affinity than apoE4 (16, 17), while apoE3 and apoE4 purified from HEK-apoE and plasma VLDL exhibit a comparable, lower affinity for A $\beta$  (17, 18, 35). That HEK-apoE assemblies exhibit functions comparable to lipoprotein-associated apoE is further suggested by several in vitro models for the role of apoE in the brain. We have demonstrated that HEK-apoE inhibits both A $\beta$ -induced neurotoxicity and glial-mediated inflammation and this inhibition is blocked by RAP (59, 60). Further, HEK-apoE3 but not HEK-apoE4 supports neurite sprouting in primary rat cortical neurons (Teter and LaDu, unpublished observations), as has been described for glial-apoE3 and glial-apoE4 particles expressed in hippocampal slice cultures from apoE transgenic animals (10). Murine glial cells secreting apoE3- but not apoE4-containing lipoproteins also promote neurite outgrowth (11). In addition, apoE-

enriched  $\beta$ -VLDL also exhibited this apoE isoform-specific effect on neurite outgrowth in a neuronal cell line, and the effect was demonstrated to require LRP (9). Thus, HEK-apoE mimics the function of a variety of lipoprotein particles including LRP receptor binding and complex formation with  $A\beta$ , functions which may further contribute to the effect of apoE on  $A\beta$ -induced neurotoxicity and neuroinflammation, as well as the isoform-specific effect of apoE on neurite outgrowth.

One of the primary functions of apoE-containing lipoproteins in the plasma is the delivery and clearance of lipid, particularly cholesterol. However, Huang and co-workers identified a  $\gamma$ -migrating, 12 nm lipid-poor apoE-containing "particle" in plasma that appears to serve as a cholesterol acceptor (41). A similar process may occur in the CNS. Following its secretion, apoE and/or apoE-containing CNS lipoproteins appear to exhibit a paracrine-like function distributing lipids via binding to cell surface apoE receptors on neurons and glia. It is possible that when apoE is acutely produced following injury in the peripheral or CNS (6, 61–63), it is secreted in lipid-poor or lipid-free forms. These apoE assemblies can then take up extracellular lipid for delivery via apoE receptors to neurons to support regeneration. In addition, apoE-containing CNS particles may also accept cholesterol from neural cells via ABCA1 transporters (64, 65). Although the in vivo roles of the LDLR and LRP in CNS apoE/lipoprotein metabolism are not clear, overexpression of LRP in CNS neurons via a transgenic approach (66) results in a significant decrease in brain apoE levels (Zerbinatti and Bu, manuscript in preparation).

Taken together, these results suggest that, in addition to lipid distribution in the CNS, apoE and LRP may play a role in the clearance of apoE/ $A\beta$  complexes (12, 14, 15, 18), similar to the clearance of  $\alpha_2$ -macroglobulin/ $A\beta$  complexes by LRP (14, 67). Although apoE3 and apoE4 exhibit a similar affinity for cell surface receptors, because apoE3 has a greater affinity for  $A\beta$ , apoE can potentially mediate the catabolism of  $A\beta$  in an isoform-specific manner. The fact that HEK-apoE is a ligand for LRP and exhibits isoform-specific binding to  $A\beta$  suggests that these apoE assemblies are a viable reagent for further investigation of the role of apoE isoform and assembly state on apoE receptor-mediated clearance of  $A\beta$ , studies that may give insights into the pathogenesis of AD. In addition, these results contribute to the growing body of evidence that the conformation of apoE, as induced by assembly state, lipidation, or experimental conditions, significantly affects the receptor specificity of apoE (57, 58). Thus, in designing future experiments on the biological role of apoE, the form of apoE is critically important to any results that are influenced by apoE receptor specificity.

## ACKNOWLEDGMENT

The authors thank Reemy Balestra and Yvonne Newhouse at the Gladstone Institute for Cardiovascular Disease for performing the LDLR binding assay (Figure 6), John Lukens and Daniel Schneider for technical assistance at the University of Chicago, Yadong Huang and Karl Weisgraber for spirited discussions and input, and Joachim Herz for kindly providing MEF cell lines.

## REFERENCES

- Mahley, R. W. (1988) Apolipoprotein E: Cholesterol transport protein with expanding role in cell biology, *Science* 240, 622–630.
- Brown, M. S., and Goldstein, J. L. (1986) A receptor-mediated pathway for cholesterol homeostasis, *Science* 232, 34–47.
- LaDu, M. J., Reardon, C. A., Van Eldik, L. J., Fagan, A. M., Bu, G., Holtzman, D., and Getz, G. S. (2000) Lipoproteins in the central nervous system, *Ann. N.Y. Acad. Sci.* 903, 167–175.
- Strittmatter, W. J., Saunders, A. M., Schmechel, D., Pericak-Vance, M., Enghild, J., Salvesen, G. S., and Roses, A. D. (1993) Apolipoprotein E: high avidity binding to  $\beta$ -amyloid and increased frequency of type 4 allele in late-onset familial Alzheimer disease, *Proc. Natl. Acad. Sci. U.S.A.* 90, 1977–1981.
- Corder, E. H., Saunders, S. M., Strittmatter, W. J., Schmechel, D. E., Gaskell, P. C., Small, G. W., Roses, A. D., Haines, J. L., and Pericak-Vance, M. A. (1993) Gene dose of apolipoprotein E type 4 allele and the risk of Alzheimer's disease in late onset families, *Science* 261, 921–923.
- Poirier, J. (1994) Apolipoprotein E in animal models of CNS injury and in Alzheimer's disease, *Trends Neurosci.* 17, 525–530.
- Horsburgh, K., McCarron, M. O., White, F., and Nicoll, J. A. (2000) The role of apolipoprotein E in Alzheimer's disease, acute brain injury and cerebrovascular disease: evidence of common mechanisms and utility of animal models, *Neurobiol. Aging* 21, 245–255.
- Nathan, B. P., Bellosta, S., Sanan, D. A., Weisgraber, K. H., Mahley, R. W., and Pitas, R. E. (1994) Differential effects of apolipoproteins E3 and E4 on neuronal growth in vitro, *Science* 264, 850–852.
- Holtzman, D. M., Pitas, R. E., Kilbridge, J., Nathan, B., Mahley, R. W., Bu, G., and Schwartz, A. L. (1995) Low density lipoprotein receptor-related protein mediates apolipoprotein E-dependent neurite outgrowth in a central nervous system-derived neuronal cell line, *Proc. Natl. Acad. Sci. U.S.A.* 92, 9480–9484.
- Teter, B., Xu, P. T., Gilbert, J. R., Roses, A. D., Galasko, D., and Cole, G. M. (2002) Defective neuronal sprouting by human apolipoprotein E4 is a gain-of-negative function, *J. Neurosci. Res.* 68, 331–336.
- Peng, D., Song, C., Reardon, C. A., Liao, S., and Getz, G. S. (2003) Lipoproteins produced by ApoE<sup>-/-</sup> astrocytes infected with adenovirus expressing human ApoE, *J. Neurochem.* 86, 1391–1402.
- Rebeck, G. W., Reiter, J. S., Strickland, D. K., and Hyman, B. T. (1993) Apolipoprotein E in sporadic Alzheimer's disease: allelic variation and receptor interactions, *Neuron* 11, 575–580.
- Koistinaho, M., Lin, S., Wu, X., Esterman, M., Koger, D., Hanson, J., Higgs, R., Liu, F., Malkani, S., Bales, K. R., and Paul, S. M. (2004) Apolipoprotein E promotes astrocyte colocalization and degradation of deposited amyloid-beta peptides, *Nat. Med.* 10, 719–726.
- Shibata, M., Yamada, S., Kumar, S. R., Calero, M., Bading, J., Frangione, B., Holtzman, D. M., Miller, C. A., Strickland, D. K., Ghiso, J., and Zlokovic, B. V. (2000) Clearance of Alzheimer's amyloid-ss(1–40) peptide from brain by LDL receptor-related protein-1 at the blood-brain barrier, *J. Clin. Invest.* 106, 1489–1499.
- Beffert, U., Aumont, N., Dea, D., Lussier-Cacan, S., Davignon, J., and Poirier, J. (1998) Beta-amyloid peptides increase the binding and internalization of apolipoprotein E to hippocampal neurons, *J. Neurochem.* 70, 1458–1466.
- LaDu, M. J., Falduto, M. T., Manelli, A. M., Reardon, C. A., Getz, G. S., and Frail, D. E. (1994) Isoform-specific binding of apolipoprotein E to  $\beta$ -amyloid, *J. Biol. Chem.* 269, 23404–23406.
- LaDu, M. J., Pederson, T. M., Frail, D. E., Reardon, C. A., Getz, G. S., and Falduto, M. T. (1995) Purification of apolipoprotein E attenuates isoform-specific binding to  $\beta$ -amyloid, *J. Biol. Chem.* 270, 9030–9042.
- Tokuda, T., Calero, M., Matsubara, E., Vidal, R., Kumar, A., Permanne, B., Zlokovic, B., Smith, J., LaDu, M. J., Rostagno, A., Frangione, B., and Ghiso, J. (2000) Lipidation of apolipoprotein E influences its isoform-specific interaction with Alzheimer's amyloid  $\beta$ -peptide, *Biochem. J.* 348, 359–365.
- Bales, K. R., Verina, T., Dodel, R. C., Du, Y., Altstiel, L., Bender, M., Hyslop, P., Johnstone, E. M., Little, S. P., Cummins, D. J., Piccardo, P., Ghetti, B., and Paul, S. M. (1997) Lack of apolipoprotein E dramatically reduces amyloid  $\beta$ -peptide deposition, *Nat. Genet.* 17, 263–264.



20. Holtzman, D. M., Bales, K. R., Tenkova, T., Fagan, A. M., Parsadanian, M., Sartorius, L. J., Macky, B., Olney, J., McKeel, D., Wozniak, D., and Paul, S. M. (2000) Apolipoprotein E isoform-dependent amyloid deposition and neuritic degeneration in a mouse model of Alzheimer's disease, *Proc. Natl. Acad. Sci. U.S.A.* 97, 2892–2897.
21. Dolev, I., and Michaelson, D. M. (2004) A nontransgenic mouse model shows inducible amyloid-beta (A $\beta$ ) peptide deposition and elucidates the role of apolipoprotein E in the amyloid cascade, *Proc. Natl. Acad. Sci. U.S.A.* 101, 13909–13914.
22. Bradley, W. A., and Gianturco, S. H. (1986) ApoE is necessary and sufficient for the binding of large triglyceride-rich lipoproteins to the LDL receptor; apoB is unnecessary, *J. Lipid Res.* 27, 40–48.
23. Dong, L. M., Innerarity, T. L., Arnold, K. S., Newhouse, Y. M., and Weisgraber, K. H. (1998) The carboxyl terminus in apolipoprotein E2 and the seven amino acid repeat in apolipoprotein E-Leiden: role in receptor-binding activity, *J. Lipid Res.* 39, 1173–1180.
24. Kowal, R. C., Herz, J., Goldstein, J. L., Esser, V., and Brown, M. S. (1989) Low density lipoprotein receptor-related protein mediates uptake of cholesteryl esters derived from apoprotein E-enriched lipoproteins, *Proc. Natl. Acad. Sci. U.S.A.* 86, 5810–5814.
25. Beisiegel, U., Weber, W., Ihrke, G., Herz, J., and Stanley, K. K. (1989) The LDL-receptor-related protein, LRP, is an apolipoprotein E-binding protein, *Nature* 341, 162–164.
26. Krieger, M., and Herz, J. (1994) Structures and functions of multiligand lipoprotein receptors: macrophage scavenger receptors and LDL receptor-related protein (LRP), *Annu. Rev. Biochem.* 63, 601–637.
27. Herz, J., Hamann, U., Rogne, S., Myklebost, O., Gausepohl, H., and Stanley, K. K. (1988) Surface location and high affinity for calcium of a 500-kD liver membrane protein closely related to the LDL-receptor suggest a physiological role as lipoprotein receptor, *EMBO J.* 7, 4119–4127.
28. Strickland, D. K., Kounnas, M. Z., and Argraves, W. S. (1995) LDL receptor-related protein: a multiligand receptor for lipoprotein and proteinase catabolism, *FASEB J.* 9, 890–898.
29. Herz, J., and Strickland, D. K. (2001) LRP: a multifunctional scavenger and signaling receptor, *J. Clin. Invest.* 108, 779–784.
30. Herz, J. (2001) The LDL receptor gene family: (un)expected signal transducers in the brain, *Neuron* 29, 571–581.
31. Willnow, T. E., Goldstein, J. L., Orth, K., Brown, M. S., and Herz, J. (1992) Low density lipoprotein receptor-related protein and gp330 bind similar ligands, including plasminogen activator-inhibitor complexes and lactoferrin, an inhibitor of chylomicron remnant clearance, *J. Biol. Chem.* 267, 26172–26180.
32. Takahashi, S., Kawarabayashi, Y., Nakai, T., Sakai, J., and Yamamoto, T. (1992) Rabbit very low density lipoprotein receptor: a low density lipoprotein receptor-like protein with distinct ligand specificity, *Proc. Natl. Acad. Sci. U.S.A.* 89, 9252–9256.
33. Kim, D. H., Iijima, H., Goto, K., Sakai, J., Ishii, H., Kim, H. J., Suzuki, H., Kondo, H., Saeki, S., and Yamamoto, T. (1996) Human apolipoprotein E receptor 2. A novel lipoprotein receptor of the low density lipoprotein receptor family predominantly expressed in brain, *J. Biol. Chem.* 271, 8373–8380.
34. Yamazaki, H., Bujo, H., Kusunoki, J., Seimiya, K., Kanaki, T., Morisaki, N., Schneider, W. J., and Saito, Y. (1996) Elements of neural adhesion molecules and a yeast vacuolar protein sorting receptor are present in a novel mammalian low density lipoprotein receptor family member, *J. Biol. Chem.* 271, 24761–24768.
35. Strittmatter, W. J., Weisgraber, K. H., Huang, D. Y., Dong, L.-Y., Salvesen, G. S., Pericak-Vance, M., Schmechel, D., Saunders, A. M., Goldgaber, D., and Roses, A. D. (1993) Binding of human apolipoprotein E to synthetic amyloid  $\beta$  peptide: isoform specific-effects and implications for late-onset Alzheimer disease, *Proc. Natl. Acad. Sci. U.S.A.* 90, 8098–8102.
36. Hu, J., Akama, K. T., Krafft, G. A., Chromy, B. A., and Van Eldik, L. J. (1998) Amyloid-beta peptide activates cultured astrocytes: morphological alterations, cytokine induction and nitric oxide release, *Brain Res.* 785, 195–206.
37. LaDu, M. J., Gilligan, S. M., Lukens, S. R., Cabana, V. G., Reardon, C. A., Van Eldik, L. J., and Holtzman, D. M. (1998) Nascent astrocyte particles differ from lipoproteins in CSF, *J. Neurochem.* 70, 2070–2081.
38. Fagan, A. M., Holtzman, D. M., Munson, G., Mathur, T., Schneider, D., Chang, L. K., Getz, G. S., Reardon, C. A., Lukens, J., Shah, J. A., and LaDu, M. J. (1999) Unique lipoproteins secreted by primary astrocytes from wild type, apoE(-/-), and human apoE transgenic mice, *J. Biol. Chem.* 274, 30001–30007.
39. Cabana, V. G., Siegel, J. N., and Sabesin, S. M. (1989) Effects of the acute phase response on the concentration and density distribution of plasma lipids and apolipoproteins, *J. Lipid Res.* 30, 39–49.
40. Bu, G., Morton, P. A., and Schwartz, A. L. (1992) Identification and partial characterization by chemical cross-linking of a binding protein for tissue-type plasminogen activator (t-PA) on rat hepatoma cells, *J. Biol. Chem.* 267, 15595–15602.
41. Huang, Y., von Eckardstein, A., Wu, S., Maeda, N., and Assmann, G. (1994) A plasma lipoprotein containing only apolipoprotein E and with gamma mobility on electrophoresis releases cholesterol from cells, *Proc. Natl. Acad. Sci. U.S.A.* 91, 1834–1838.
42. Narita, M., Holtzman, D. M., Fagan, A. M., LaDu, M. J., Yu, L., Han, X., Gross, R. W., Bu, G., and Schwartz, A. L. (2002) Cellular catabolism of lipid poor apolipoprotein E via cell surface LDL receptor-related protein, *J. Biochem.* 132, 743–749.
43. Bu, G., and Schwartz, A. L. (1998) RAP, a novel type of ER chaperone, *Trends Cell Biol.* 8, 272–276.
44. Mahley, R. W., Weisgraber, K. H., Hussain, M. M., Greenman, B., Fisher, M., Vogel, T., and Gorecki, M. (1989) Intravenous infusion of apolipoprotein E accelerates clearance of plasma lipoproteins in rabbits, *J. Clin. Invest.* 83, 2125–2130.
45. Ji, Z. S., Dichek, H. L., Miranda, R. D., and Mahley, R. W. (1997) Heparan sulfate proteoglycans participate in hepatic lipase and apolipoprotein E-mediated binding and uptake of plasma lipoproteins, including high-density lipoproteins, *J. Biol. Chem.* 272, 31285–31292.
46. Schwartz, M. W., Sipols, A., Kahn, S. E., Lattemann, D. F., Taborsky, G. J., Jr., Bergman, R. N., Woods, S. C., and Porte, D., Jr. (1990) Kinetics and specificity of insulin uptake from plasma into cerebrospinal fluid, *Am. J. Physiol.* 259, E378–E383.
47. Westerlund, J. A., and Weisgraber, K. H. (1993) Discrete carboxyl-terminal segments of apolipoprotein E mediate lipoprotein association and protein oligomerization, *J. Biol. Chem.* 268, 15745–15750.
48. Chan, W., Fornwald, J., Brawner, M., and Wetzel, R. (1996) Native complex formation between apolipoprotein E isoforms and the Alzheimer's disease peptide A $\beta$ , *Biochemistry* 35, 7123–7130.
49. Yokoyama, S., Kawai, Y., Tajima, S., and Yamamoto, A. (1985) Behavior of human apolipoprotein E in aqueous solutions and at interfaces, *J. Biol. Chem.* 260, 16375–16382.
50. Weisgraber, K. H. (1994) Apolipoprotein E: structure-function relationships, *Adv. Protein Chem.* 45, 249–302.
51. Perugini, M. A., Schuck, P., and Howlett, G. J. (2000) Self-association of human apolipoprotein E3 and E4 in the presence and absence of phospholipid, *J. Biol. Chem.* 275, 36758–36765.
52. Dergunov, A. D., Shuvaev, V. V., and Yanushevskaja, E. V. (1992) Quaternary structure of apolipoprotein E in solution: fluorimetric, chromatographic and immunochemical studies, *Biol. Chem. Hoppe-Seyler* 373, 323–331.
53. Lund-Katz, S., Weisgraber, K. H., Mahley, R. W., and Phillips, M. C. (1993) Conformation of apolipoprotein E in lipoproteins, *J. Biol. Chem.* 268, 23008–23015.
54. Innerarity, T. L., and Mahley, R. W. (1978) Enhanced binding by cultured human fibroblasts of apo-E-containing lipoproteins as compared with low density lipoproteins, *Biochemistry* 17, 1440–1447.
55. Innerarity, T., Hui, D., Bersot, T., and Mahley, R. W. (1986) Type III hyperlipoproteinemia: a focus on lipoprotein receptor-apolipoprotein E2 interactions, *Adv. Exp. Med. Biol.* 201, 273–288.
56. Kowal, R. C., Herz, J., Weisgraber, K. H., Mahley, R. W., Brown, M. S., and Goldstein, J. L. (1990) Opposing effects of apolipoproteins E and C on lipoprotein binding to low density lipoprotein receptor-related protein, *J. Biol. Chem.* 265, 10771–10779.
57. Ruiz, J., Kouivaskaia, D., Migliorini, M., Robinson, S., Saenko, E. L., Gorlatova, N., Li, D., Lawrence, D., Hyman, B. T., Weisgraber, K. H., and Strickland, D. K. (2005) Characterization of the apoE isoform binding properties of the VLDL receptor reveal marked differences from LRP and the LDL receptor, *J. Lipid Res.* 46, 1721–1731.
58. Fryer, J. D., Demattos, R. B., McCormick, L. M., O'Dell, M. A., Spinner, M. L., Bales, K. R., Paul, S. M., Sullivan, P. M., Parsadanian, M., Bu, G., and Holtzman, D. M. (2005) The low-density lipoprotein receptor regulates the level of CNS human and murine apolipoprotein E but does not modify amyloid plaque pathology in PDAPP mice, *J. Biol. Chem.* 280, 25754–25759.

59. Jordan, J., Galindo, M. F., Miller, R. J., Reardon, C. A., Getz, G. S., and LaDu, M. J. (1998) Isoform-specific effect of apolipoprotein E on cell survival and beta-amyloid-induced toxicity in rat hippocampal pyramidal neuronal cultures, *J. Neurosci.* 18, 195–204.
60. LaDu, M. J., Shah, J. A., Reardon, C. A., Getz, G. S., Bu, G., Hu, J., Guo, L., and Van Eldik, L. J. (2001) Apolipoprotein E and apolipoprotein E receptors modulate A beta-induced glial neuroinflammatory responses, *Neurochem. Int.* 39, 427–434.
61. Ignatius, M. J., Gebicke-Harter, P. J., Skene, J. H. P., Schilling, J. W., Weisgraber, K. H., Mahley, R. W., and Shooter, E. M. (1986) Expression of apolipoprotein E during nerve degeneration and regeneration, *Proc. Natl. Acad. Sci. U.S.A.* 83, 1125–1129.
62. Holtzman, D. M., and Fagan, A. M. (1998) Potential role of apoE in structural plasticity in the nervous system: Implications for diseases of the central nervous system, *Trends Cardiovasc. Med.* 8, 250–255.
63. Boyles, J. K., Zoellner, C. D., Anderson, L. J., Kosik, L. M., Pitas, R. E., Weisgraber, K. H., Hui, D. Y., Mahley, R. W., Gebicke-Harter, P. J., Ignatius, M. J., and Shooter, E. M. (1989) A role for apolipoprotein E, apolipoprotein A-I, and low density lipoprotein receptors in cholesterol transport during regeneration and remyelination of the rat sciatic nerve, *J. Clin. Invest.* 83, 1015–1031.
64. Wahrle, S. E., Jiang, H., Parsadanian, M., Legleiter, J., Han, X., Fryer, J. D., Kowalewski, T., and Holtzman, D. M. (2004) ABCA1 is required for normal central nervous system ApoE levels and for lipidation of astrocyte-secreted apoE, *J. Biol. Chem.* 279, 40987–40993.
65. Hirsch-Reinshagen, V., Zhou, S., Burgess, B. L., Bernier, L., McIsaac, S. A., Chan, J. Y., Tansley, G. H., Cohn, J. S., Hayden, M. R., and Wellington, C. L. (2004) Deficiency of ABCA1 impairs apolipoprotein E metabolism in brain, *J. Biol. Chem.* 279, 41197–41207.
66. Zerbinatti, C. V., Wozniak, D. F., Cirrito, J., Cam, J. A., Osaka, H., Bales, K. R., Zhuo, M., Paul, S. M., Holtzman, D. M., and Bu, G. (2004) Increased soluble amyloid-beta peptide and memory deficits in amyloid model mice overexpressing the low-density lipoprotein receptor-related protein, *Proc. Natl. Acad. Sci. U.S.A.* 101, 1075–1080.
67. Narita, M., Holtzman, D. M., Schwartz, A. L., and Bu, G. (1997) Alpha2-macroglobulin complexes with and mediates the endocytosis of beta-amyloid peptide via cell surface low-density lipoprotein receptor-related protein, *J. Neurochem.* 69, 1904–1911.

BI051765S